

# Semantic-Enhanced Time-Series Forecasting via Large Language Models

Hao Liu<sup>1</sup> Chun Yang<sup>1</sup>, Zhang xiaoxing<sup>2</sup>, Xiaobin Zhu<sup>1</sup>

<sup>1</sup>University of Science and Technology Beijing

<sup>2</sup>Yizhi, China Telecom

d202410441@xs.ustb.edu.cn, chunyang@ustb.edu.cn, xiaobinzh@ustb.edu.cn, zhangxx7@chinatelecom.cn

## Abstract

Time series forecasting plays a significant role in finance, energy, meteorology, and IoT applications. Recent studies have leveraged the generalization capabilities of large language models (LLMs) to adapt to time series forecasting, achieving promising performance. However, existing studies focus on token-level modal alignment, instead of bridging the intrinsic modality gap between linguistic knowledge structures and time series data patterns, greatly limiting the semantic representation. To address this issue, we propose a novel Semantic-Enhanced LLM (SE-LLM) that explores the inherent periodicity and anomalous characteristics of time series to embed into the semantic space to enhance the token embedding. This process enhances the interpretability of tokens for LLMs, thereby activating the potential of LLMs for temporal sequence analysis. Moreover, existing Transformer-based LLMs excel at capturing long-range dependencies but are weak at modeling short-term anomalies in time-series data. Hence, we propose a plugin module embedded within self-attention that models long-term and short-term dependencies to effectively adapt LLMs to time-series analysis. Our approach freezes the LLM and reduces the sequence dimensionality of tokens, greatly reducing computational consumption. Experiments demonstrate the superiority performance of our SE-LLM against the state-of-the-art (SOTA) methods.

## Introduction

Time series forecasting has widespread applications in various tasks, such as finance, energy, meteorology, and industrial IoT (Liu et al. 2016; Arslan 2022; Sherstinsky 2020). Recently, Transformer-based LLMs (Radford et al. 2019; Devlin et al. 2019; Yang et al. 2024a; Touvron et al. 2023) are prevalent in time series forecasting (Jin et al. 2024; Liu et al. 2024b, 2025; Hu et al. 2025) by integrating multi-domain knowledge to model temporal dependencies, thereby enhancing time series analysis effectively.

Time series data fundamentally differs from linguistic structures in nature. Existing methods often convert temporal information into textual prompts to activate the potential of LLMs. GPT4mTS (Jia et al. 2024a) introduces a prompt-based framework that jointly processes temporal data and textual information. Zhou et al. (Zhou et al. 2023) processed time-series data by randomly initializing the embedding layer and directly performing serialized analysis through frozen LLMs. However, the inherent modality gap

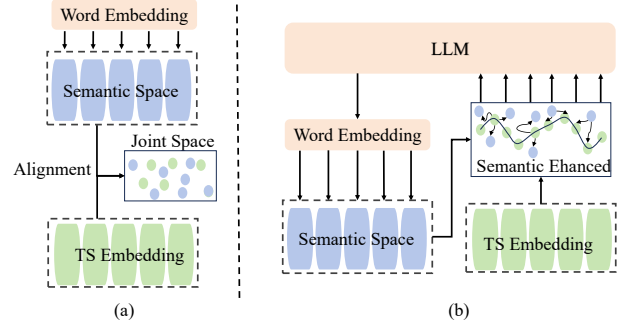


Figure 1: (a) The input time series is mapped to obtain time series (TS) Embeddings. Next, the feature space is aligned with the semantic space derived from the pre-trained word token embedding. (b) Temporal patterns are injected into the joint space and use implicit prompts to LLM for forecasting.

between temporal and linguistic data resulted in low-quality embeddings. In this regard, LLM4TS (Chang, Peng, and Chen 2025) introduces a unified framework that fuses token, positional, and temporal embeddings to maintain modality consistency. Time-LLM (Jin et al. 2024) converts time-series data into text prototype representations and integrates textual prompts to enhance time series analysis. Meanwhile, S2IP-LLM (Pan et al. 2024a) incorporates time-series data into LLM's semantic space as prompts, compensating for the lack of textual prompts. However, incorporating textual information may introduce noise (Liu et al. 2025), and the text descriptions incur additional computational cost (Lin et al. 2024; Ma et al. 2023; Shang et al. 2024).

Current most LLM-based methods mainly focus on token-level alignment (Hu et al. 2025), as shown in Fig. 1 (a) (Pan et al. 2024a; Liu et al. 2025). The joint space serves as an implicit prompt, guiding the LLM in conducting time series forecasting. However, the semantic tokenization eliminates the dependency on auxiliary textual descriptions, leading to noise and computational costs (Jin et al. 2024). To address these limitations, our analysis identifies a critical oversight in existing LLM-based approaches (Jin et al. 2024; Liu et al. 2024b; Chang, Peng, and Chen 2025; Zhou et al. 2023). Regarding the semantic space composed of tokens and time steps, we propose the Temporal Semantic Cross-Correlation

(TSCC) Module to obtain enhanced semantics that represent temporal patterns, emphasize anomaly and de-anomaly patterns, thereby enhancing the interpretability of the token embeddings, as shown in Fig. 1 (b).

Although we provide semantic guidance with high interpretability from LLMs, there exists an inherent difference between LLMs' understanding of linguistic knowledge and time series data, making the modal gap difficult to bridge. In summary, we propose Semantic-Enhanced LLM, a novel framework that enhances LLM for time series forecasting with two key components: the Temporal-Semantic Cross-Correlation (TSCC) module and the Time-Adapter architecture. The TSCC captures cross-correlation of temporal embedding and semantic space with temporal dependencies and channel-wise relationships, which embed into token embedding to adapt LLM to temporal features. The Time-Adapter enhances forecasting capability by overcoming the limitation of LLMs in modeling both short-term and long-term dependencies based on historical time segments. This enables pretrained LLMs to forecast time series effectively. Our main contributions are four-fold:

- We introduce a novel SE-LLM to bridge the inherent modal differences between time series and language data, activating the generalization capability of LLMs for time-series analysis.
- We propose a novel Temporal-Semantic-Cross-Correlation (TSCC) module to enhance token embedding by endowing semantic information with temporal patterns, which improves temporal analysis.
- We propose a Time-Adapter to bridge the modality gap between LLMs and time-series data, effectively modeling both long-term dependencies and short-term patterns.
- Extensive experiments verify the superior performance and efficiency of our SE-LLM.

## Related Works

### Time Series Forecasting

Traditional time series forecasting methods, such as ARIMA (Liu et al. 2016) and Prophet (Arslan 2022), often relied on statistical and classical machine learning techniques. The rise of deep learning brought Recurrent Neural Networks (RNNs)(Sherstinsky 2020; Qin et al. 2017; Yeo et al. 2018; Khaldi et al. 2023), which excelled at modeling temporal dependencies. Long Short-Term Memory (LSTM) networks(Kong et al. 2025; Zaheer et al. 2023) improved RNNs by addressing vanishing gradients and long-range dependencies . Advances PGN (Jia et al. 2024b) further enhanced long-term temporal relationship modeling, and improved computational efficiency. Concurrently, Graph Neural Networks (GNNs)(Cao et al. 2020; Pan et al. 2024b; Deng et al. 2020) excelled at capturing spatial and structural dependencies in spatiotemporal contexts. Recently, Transformer-based architectures(Chen et al. 2021; Zhang and Yan 2023; Wang et al. 2024) have dominated due to their ability to capture global temporal patterns. However, these models struggle with generalizability and flexibility in highly dynamic, real-world time series analysis.

### LLM-based Time Series Forecasting

Recently, LLMs (Radford et al. 2019; Touvron et al. 2023; Zhang et al. 2022; DeepSeek-AI et al. 2024; Yang et al. 2024a) have developed rapidly, and demonstrated significant potential in advancing time-series forecasting. Gruver *et al.* (Gruver et al. 2023) and Xue *et al.* (Xue and Salim 2023) reformulated forecasting as a sentence-to-sentence translation task to bridge the modality gap. Time-LLM (Jin et al. 2024) leverages token-level embedding as a prompt to enhance the textual description to enhance LLM's understanding of temporal concepts. Pan *et al.* (Pan et al. 2024a) integrate semantic space with embedding as a prompt to guide LLM. Liu *et al.* (Liu et al. 2025) indicate that the embedding of textual information is weak, and they proposed an entangled reliable embedding. Hu *et al.* (Hu et al. 2025) introduced DECA, which utilizes Graph Neural Networks (GNNs) to ensure structural and logical alignment. AutoTimes (Liu et al. 2024b) explored autoregressive forecasting with timestamp embedding to improve LLM's performance. Notably, the aforementioned studies and most research (Jia et al. 2024a) employ a frozen LLM approach for time series learning, indicating that LLMs have already acquired rich general semantic recognition capabilities during the pre-training weight. If all parameters are directly fine-tuned, these general capabilities may be compromised, leading to unstable performance in time series tasks. Current research merely leverages the generalization ability of LLMs for downstream tasks, suggesting that the inherent architecture of LLMs is not well-suited for time series forecasting.

### Adapter-based LLM Fine-Tune

Existing methods show that fine-tuning LLMs (Jin et al. 2024; Zhou et al. 2023; Gruver et al. 2023) not only consumes computational resources but also degrades forecasting performance across data from different domains. Adapter-based fine-tuning techniques (Hu et al. 2022; Guo et al. 2024; Zhang et al. 2023; Zhang, Zhu, and Gao 2025; Lester, Al-Rfou, and Constant 2021) have demonstrated efficient adaptation to task-specific distributions in various task (Liu, Zeng, and Ren 2024; Chen, Jie, and Ma 2024; Mu et al. 2024). Empirical studies, such as Gupta *et al.*(Gupta et al. 2024), validate the effectiveness of LoRA-style fine-tuning in boosting time-series forecasting performance. AutoTimes(Liu et al. 2024b) incorporates LoRA (Hu et al. 2022) into GPT-2 (Radford et al. 2019), achieving substantial improvements in long-range prediction scenarios. However, the success of these fine-tuning techniques is highly contingent upon algorithmic design choices (Pan et al. 2024a; Zhou et al. 2023; Jin et al. 2024), and the transferability of these methods across diverse time-series domains remains unclear. We contend that current adapters, while enhancing LLMs' understanding of semantic structures, are not designed to capture temporal patterns effectively. In contrast, the Time-Adapter is specifically designed to model short-term and long-term dependencies, enabling LLMs to better adapt to temporal forecasting tasks.

## Methods

### The Overview of SE-LLM

The proposed SE-LLM model consists of two primary components: the TSCC and the Time-Adapter, as depicted in Fig. 2. The process begins with the input sequence, a time series data matrix with batch size  $B$  and sequence length  $L$ . A sliding window operation is applied to partition the temporal dimension into smaller segments, restructuring the representation and reducing computational complexity from  $\mathcal{O}(L^2)$  to  $\mathcal{O}(N^2K)$ , where  $\mathbf{T} \rightarrow \tilde{\mathbf{T}}$ ,  $\tilde{\mathbf{T}} \in \mathbb{R}^{B \times N \times K}$ . This design reduces self-attention and feed-forward network complexities, improving the model's efficiency.

**TS Embedding.** The temporal representation is passed through the Time Encoder module, which projects the data into a high-dimensional TS Embeddings, which can be formulated as:

$$\mathbf{H} = \mathcal{F}_2 \left( \sigma \left( \mathcal{F}_1(\tilde{\mathbf{T}}) \right) \right), \quad (1)$$

where  $\mathbf{H} \in \mathbb{R}^{B \times N \times C}$ ,  $\mathcal{F}_1, \mathcal{F}_2$  is linear model,  $\sigma$  is activation. This projection captures more expressive features of the temporal patterns within the data.

**Semantic Space.** The semantic space is the semantic embedding obtained by mapping the word embedding of a large language model through a linear layer, which we collectively refer to as the semantic space. Specifically, we map the Word Embedding layer from  $l_1 \in \mathbb{R}^{L_1 \times C}$  to  $l_2 \in \mathbb{R}^{K \times C}$  (Fang et al. 2025).

The pre-trained word embeddings from LLM are used as general features, and a linear transformation is applied to transfer the features to a new semantic space, allowing the model to match the time series of the TS Embeddings. We input both the semantic space and features into the TSCC to obtain enhanced semantics, as shown in Fig. 2(b). Following this, the LLM embeds Time-Adapter into the Multi-Head Attention to further refine the model's ability to understand temporal patterns in the time series data, as shown in Fig. 2(c). This component enhances the overall temporal pattern recognition by integrating additional contextual information, enabling better forecasting performance. Finally, the Decoder component decodes the output from the LLM to produce the final prediction, which can be formulated as:

$$\mathbf{O} = \mathcal{F}_2 \left( \sigma \left( \mathcal{F}_1(\mathbf{Y}) \right) \right), \quad (2)$$

where  $\mathbf{O} \in \mathbb{R}^{B \times N \times K}$ ,  $\mathbf{Y} \in \mathbb{R}^{B \times N \times C}$  is the LLM's output.

### Temporal-Semantic Cross-Correlation

Fig. 3 is the architecture of the TSCC module. The core of this module is to infuse temporal patterns into the joint space. Firstly, we align the temporal embeddings with the semantic space through a cross-attention mechanism (Jin et al. 2024; Liu et al. 2025; Chang, Peng, and Chen 2025).

**Cross-Modality Alignment.** The Cross-Domain Attention Mechanism is capable of dynamically capturing complex associations between different modalities, and achieving efficient fusion through adaptive weight allocation. Therefore, this paper employs Cross Attention to align temporal embeddings with the semantic space, thereby obtaining output

$\mathbf{C} \in \mathbb{R}^{B \times N \times C}$ . This can be formulated as:

$$\mathbf{C} = \text{CrossAttn}(l_2, H). \quad (3)$$

Further, we take the mean along the batch and sequence dimension to element-wise sum with  $l_2$  to obtain  $\mathbf{S} \in \mathbb{R}^{K \times C}$ . The purpose is to facilitate the alignment of temporal embeddings while enriching the representation of spatial information (Fang et al. 2022).

**The Modified VAE Module.** In time series analysis, non-stationary information refers to the time-varying statistical properties of the sequence. Non-stationarity lead to inaccurate model parameter estimation and increased prediction bias. Correctly identifying and handling non-stationarity is a crucial step in time series modeling, directly affecting the accuracy and reliability of predictions.

We employ a Variational Autoencoder (VAE) (Cemgil et al. 2020) to reconstruct the mean and variance in a joint space, comprehensively capturing the statistical characteristics of the sequences. Specifically, we utilize the VAE module to model the underlying stochastic process of noise in temporal data, which refer to Algorithm 1, where  $\mathbf{DC}$  represents the latent noise component separated from the joint space,  $\mathbf{DA}$  is the denoising component, which contains information such as periodic or trends.

---

#### Algorithm 1: Variational Autoencoder (VAE) Module

---

**Require:** Cross-attention output  $\mathbf{C} \in \mathbb{R}^{B \times N \times C}$

**Ensure:** Decomposed anomaly  $\mathbf{DC}$  and de-anomalous component  $\mathbf{DA}$

- 1: **Latent Feature Projection:**  $\mathbf{V} \leftarrow \sigma(\mathcal{F}_e(\mathbf{C}))$ , where  $\mathcal{F}_e$ : Linear mapping from  $\mathbb{R}^C \rightarrow \mathbb{R}^n$
- 2: **Latent Distribution Estimation:**  $\mu, \log \sigma^2 \leftarrow \mathcal{F}_\mu(\mathbf{V}), \mathcal{F}_\sigma(\mathbf{V})$ , where  $\mathcal{F}_\mu, \mathcal{F}_\sigma$ : Linear mapping from  $\mathbb{R}^n \rightarrow \mathbb{R}^m$
- 3: **Reparameterization Trick:** Sample from latent space,  $\mathbf{z} \leftarrow \mu + \epsilon \odot \exp(0.5 \cdot \log \sigma^2)$ ,  $\epsilon \sim \mathcal{N}(0, \mathbf{I})$
- 4: **Reconstruction:** Decode latent variable to recover input,  $\hat{\mathbf{C}} \leftarrow \mathcal{F}_d(\mathbf{z})$ ,  $\mathcal{F}_d : \mathbb{R}^m \rightarrow \mathbb{R}^n \rightarrow \mathbb{R}^C$
- 5: **Anomaly Decomposition:**  $\mathbf{DC} = \mathbf{C} - \hat{\mathbf{C}}, \mathbf{DA} = \hat{\mathbf{C}}, \mathbf{DC} \in \mathbb{R}^{B \times N \times C}, \mathbf{DA} \in \mathbb{R}^{B \times N \times C}$

---

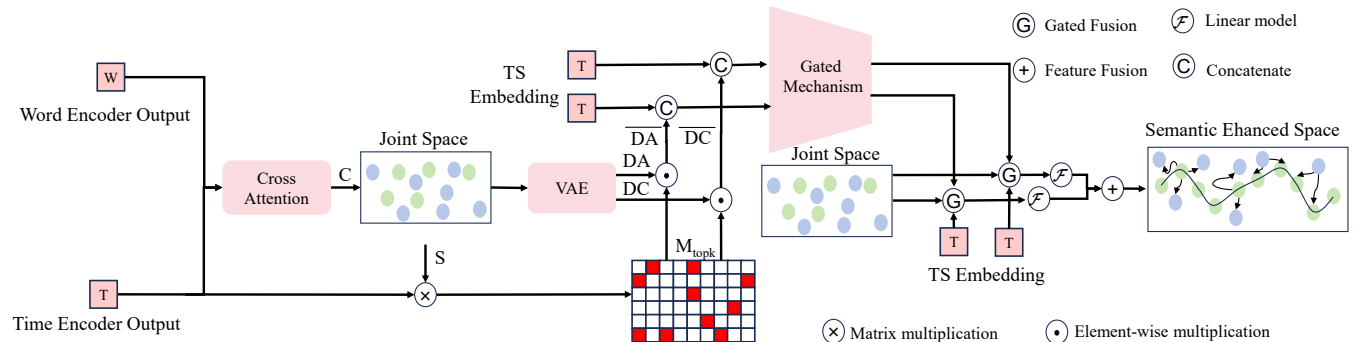
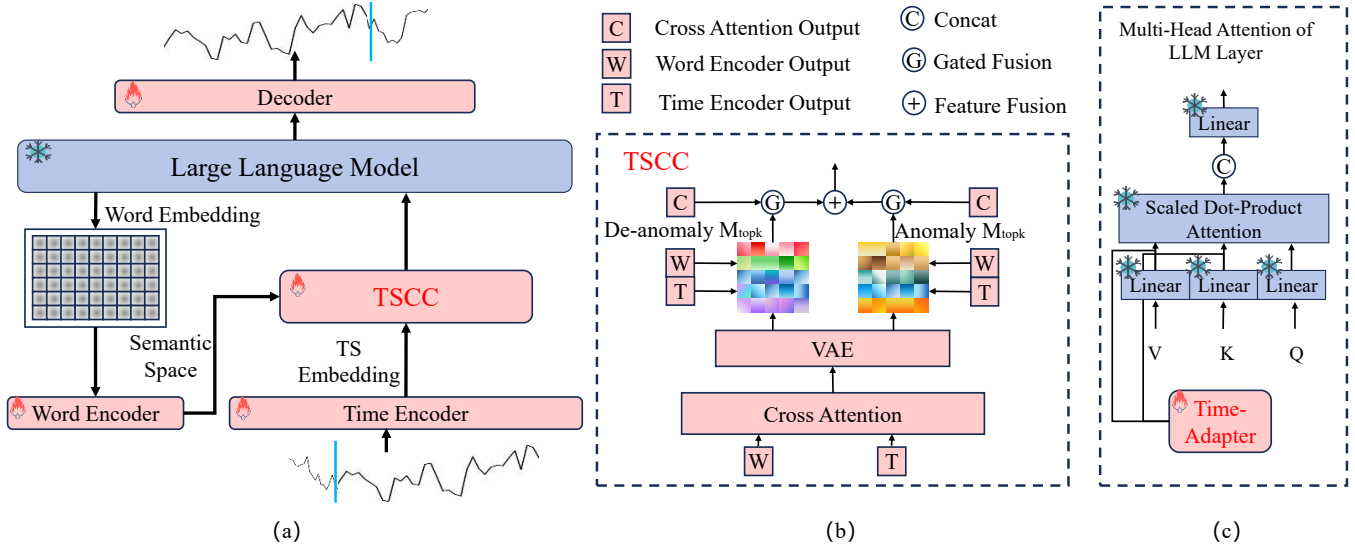
Subsequently, the cross-correlation matrix  $\mathbf{M} \in \mathbb{R}^{B \times K}$  is computed via standardization over both temporal and semantic features, which can be formulated as:

$$\mathbf{M} = \frac{\mathbf{H} - \mu_{\mathbf{H}}}{\sigma_{\mathbf{H}}} \times \frac{\mathbf{S}^T - \mu_{\mathbf{S}}}{\sigma_{\mathbf{S}}}. \quad (4)$$

Followed by a top-K (Liu, Zeng, and Ren 2024) filtering mechanism to select the most strongly correlated positions and weighted to the output of VAE to endow both anomaly and de-anomaly semantic regions with a temporal TS Embeddings that exhibits strong correlations. It can be formulated as:

$$\overline{\mathbf{DA}} = \mathbf{DA} \cdot \frac{1}{n} \sum_{i=1}^n \mathcal{P}(S_i, m_{top_k}^i), \quad (5)$$

$$\overline{\mathbf{DC}} = \mathbf{DC} \cdot \frac{1}{n} \sum_{i=1}^n \mathcal{P}(S_i, m_{top_k}^i), \quad (6)$$



where  $\overline{DC}$  represents enhanced anomaly semantics reconstructed by the VAE module from the joint space,  $\overline{DA}$  represents enhanced de-anomaly semantics, the  $\overline{DA}, \overline{DC} \in \mathbb{R}^{B \times N \times C}$ .  $\mathcal{P}$  represents the matrix in the semantic space corresponding to the indices of the top-k positions in the cross-correlation matrix.

**Channel Dependency Enhancement.** The aforementioned enhanced semantics are learned by integrating the TS Embeddings of time series data. To prevent the loss of feature information, we further acquire channel dependencies based on the enhanced semantics modeled along the temporal dimension. Specifically, we concatenate the TS Embeddings and the  $\overline{DA}, \overline{DC}$ , that share information across channel dimensions. We employ a Multi-Layer Perceptron (MLP) for attention extraction, perform channel enhancement on the enhanced semantics in the channel dimension, which can be formulated as :

$$\text{Attn}_a = \text{MLP}([H, \overline{DA}]), \quad (7)$$

where  $\overline{DC}$  has same processed to get  $\text{Attn}_c$ , and we will

mainly focus on introducing  $\overline{DA}$ .

The **Attn** incorporates region weights that model the TS Embeddings from both channel and sequence dimensions, making it sensitive to temporal patterns. We employ a gating mechanism to integrate the semantic space and the TS Embeddings, thereby endowing the joint space with temporal patterns, it can be formulated as:

$$\mathbf{GA} = \text{Attn}_a \odot S^T + (1 - \text{Attn}_a) \odot H. \quad (8)$$

The resulting embeddings are enriched with semantic information that reflects temporal patterns. Finally, the de-anomalization ( $\mathbf{GA} \in \mathbb{R}^{B \times N \times C}$ ) and anomaly ( $\mathbf{GC} \in \mathbb{R}^{B \times N \times C}$ ) representations are mapped through a linear layer for alignment and fused to generate a unified semantic representation, which is more interpretable and suitable for LLMs analysis. It can be formulated as:

$$\mathbf{Y} = \text{LLM}(\mathbf{GA} + \mathbf{GC}). \quad (9)$$

## Time-Adapter

LLMs excel at text generation, semantic understanding, and contextual reasoning. But their Transformer architecture is inherently designed for serialized textual input, soft-prompting approach still fails to bridge the modality gap. From a structural perspective, the self-attention mechanism in Transformers can directly capture long-range dependencies, enabling global analysis of time series. However, it lacks localized modeling for short-term periodicity and anomalous features. To address this issue, we propose Time-Adapter (Fig. 4), a modular component embedded into LLMs, to enhance temporal modeling. Time-Adapter explicitly captures long-term and short-term dependencies, compensating for the Transformer’s inherent weaknesses in temporal pattern extraction.

Specifically, building upon LoRA (Hu et al. 2022), we replace the low-rank matrix with dual linear layers and introduce two parallel paths incorporating LSTM (Hochreiter and Schmidhuber 1997) units. These paths process temporal dependencies by leveraging long-range information from the Transformer’s architecture through nonlinear transformations, thereby equipping the model with temporal data-handling capabilities during training.

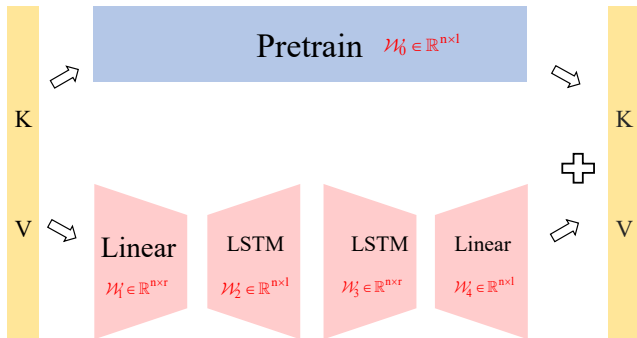


Figure 4: The architecture of Time-Adapter, a modular enhancement designed to improve the temporal modeling capabilities of LLMs. It comprises two linear layers and two parallel LSTM modules, enabling effective capture of both long-term and short-term temporal dependencies.

Our method consists of three key operations executed sequentially. First, a **Low-rank Projection** is applied, where a linear layer learns a low-rank matrix to reduce the input dimensionality. Then the **Long-term Dependency Modeling**, in which an LSTM (Zhang et al. 2022) maps the compressed features to a high-dimensional space, effectively capturing long-term temporal patterns. Finally, **Short-term Dependency Modeling** is performed, where a second LSTM processes the high-dimensional representation via a reverse projection (high-to-low mapping), isolating localized short-term dynamics. Finally, a linear layer integrates these refined temporal dependencies into the key ( $k \in \mathbb{R}^{B \times N \times C}$ ) and value ( $v \in \mathbb{R}^{B \times N \times C}$ ) matrices of the self-attention mechanism, enhancing their capacity to model temporal relationships.

## Experiments

**Baseline.** The experiments were conducted and compared with SOTA methods, using TimeMixer++ (Wang et al. 2025b) and AutoTimes (Liu et al. 2024b) as the high-performance baselines for evaluation. The algorithms involved in all the experiments are TimeMOE (Shi et al. 2025), CSFormer (Wang et al. 2025a), Time-CMA (Liu et al. 2025), Time-LLM (Jin et al. 2024), LLM-TS (Chen et al. 2025), iTransformer (Liu et al. 2024a), DLinear (Zeng et al. 2023), Time-VLM (Zhong et al. 2025), S2IP-LLM (Pan et al. 2024a), PatchTST (Nie et al. 2023), TimesNet (Wu et al. 2023), FEDFormer (Yang et al. 2024b), Informer (Zhou et al. 2021), Reformer (Kitaev, Kaiser, and Levskaya 2020), Koopa (Liu et al. 2023), and FPT (Zhou et al. 2023), some of which serve as supplementary references.

**Datasets.** We adopted publicly available benchmarks in four research domains: long-term forecasting, short-term forecasting, zero-shot forecasting and in-context forecasting (Liu et al. 2024b). The experimental datasets comprised: ETTh (Zhou et al. 2021), ETTm (Zhou et al. 2021), Weather (Chen et al. 2021), ECL (Chen et al. 2021), Traffic (Chen et al. 2021), Solar (Lai et al. 2018), M3 (Wu et al. 2023), and M4 (Makridakis, Spiliotis, and Assimakopoulos 2020) datasets. The detailed introduction refers to the **Appendix**.

## Experiment Results

**Long-Term Forecasting.** Long-term forecasting encounters formidable challenges, including trend drift, abrupt structural shifts, and noise interference, making it a representative research area. Consequently, the long-term forecasting results are shown in Table 1. The experimental results demonstrate that our method surpasses current SOTA methods on the ETTh1, Traffic, ECL, and Solar datasets. Notably, on the Traffic dataset, our approach achieves a 4.4% reduction in Mean Square Error (MSE) compared to SOTA methods. The data is missing because the algorithm’s design is incompatible with this dataset for testing purposes. There are missing results in the experiments because some studies did not provide the source code, and the algorithms were not suitable for the given dataset.

**Short-Term Forecasting.** It refers to predicting target variables within a relatively brief future time horizon. We have meticulously selected algorithms suitable for short-term forecasting for comparison. SE-LLM was compared with the SOTA models in short-term forecasting on the M4 dataset, as shown in Table 2, and the results demonstrated that we achieved the best performance. Our method achieved a 0.26% reduction in Symmetric Mean Absolute Percentage Error (SMAPE), a 0.94% decline in Mean Absolute Scaled Error (MASE), and a 0.47% decrease in Quantile-Weighted Absolute Error (QWA) relative to the second best.

**Zero-Shot forecasting.** The TSCC module employs a VAE to construct simulated noisy data, enabling the learning of latent distribution characteristics in time series and generating diverse synthetic samples. This approach enhances the model’s generalization capability for unseen data in zero-shot prediction scenarios, making it suitable for forecasting

Models		SE-LLM		TimeXier++ 2025		TimeMOE 2025		CSFormer 2025		Time-CMA 2025		LLM-TS 2025		AutoTimes-GPT2 2024		Time-LLM 2024		iTransformer 2024		DLinear 2023			
Datasets	Metrics	MSE	MAE	MSE	MAE	MSE	MAE	MSE	MAE	MSE	MAE	MSE	MAE	MSE	MAE	MSE	MAE	MSE	MAE				
ETTh1	96	0.352	0.393	0.375	0.404	<b>0.349</b>	<b>0.379</b>	0.372	0.394	0.366	0.396	0.403	0.420	0.360	0.397	0.398	0.410	0.387	0.418	0.375	0.399		
	192	<b>0.378</b>	<b>0.411</b>	0.415	0.436	0.395	<u>0.413</u>	0.420	0.425	0.401	0.420	0.440	0.441	<u>0.391</u>	0.419	0.451	0.440	0.416	0.437	0.405	0.416		
	336	<b>0.391</b>	<b>0.420</b>	0.442	0.451	0.447	0.453	0.453	0.440	0.412	<u>0.431</u>	0.471	0.457	<u>0.408</u>	0.432	0.473	0.451	0.434	0.450	0.439	0.443		
	720	<b>0.402</b>	<b>0.437</b>	0.482	0.482	0.457	0.462	0.470	0.470	<u>0.406</u>	<b>0.427</b>	0.503	0.487	0.429	0.452	0.469	0.470	0.447	0.473	0.472	0.490		
	Avg	<b>0.381</b>	<b>0.415</b>	0.429	0.443	0.412	0.426	0.429	0.432	<u>0.396</u>	0.419	0.454	0.451	0.397	0.425	0.448	0.443	0.421	0.445	0.423	0.437		
Weather	96	0.150	<b>0.200</b>	0.150	<b>0.202</b>	0.198	0.288	0.168	0.217	0.161	0.205	0.166	0.217	0.158	0.208	<b>0.149</b>	<b>0.200</b>	0.174	0.225	0.152	0.237		
	192	<b>0.194</b>	<b>0.243</b>	0.196	<u>0.244</u>	0.225	0.312	0.213	0.257	0.199	0.249	0.229	0.269	0.207	0.264	<u>0.195</u>	<b>0.243</b>	0.227	0.268	0.220	0.282		
	336	<u>0.247</u>	<b>0.285</b>	0.248	<b>0.285</b>	0.293	0.348	0.272	0.298	0.267	0.2900	0.278	0.302	0.262	0.298	<b>0.245</b>	<b>0.282</b>	0.290	0.309	0.265	0.319		
	720	0.323	0.339	<b>0.316</b>	<b>0.332</b>	0.427	0.428	0.346	0.347	0.343	0.341	0.354	0.351	0.342	0.353	0.318	0.338	0.374	0.360	0.323	0.362		
	Avg	0.229	0.267	<u>0.228</u>	<b>0.266</b>	0.288	0.344	0.250	0.280	0.243	0.271	0.257	0.285	0.242	0.281	<b>0.227</b>	<b>0.266</b>	0.266	0.291	0.240	0.300		
Traffic	96	<b>0.350</b>	<b>0.243</b>	0.367	0.266	—	—	—	—	—	—	—	—	0.587	0.315	0.369	<u>0.257</u>	0.373	0.280	<u>0.363</u>	0.259	0.410	0.282
	192	<b>0.373</b>	<b>0.254</b>	0.379	0.364	—	—	—	—	—	—	—	—	0.612	0.326	0.394	0.268	0.390	0.288	0.383	0.267	0.423	0.287
	336	<b>0.390</b>	<b>0.263</b>	0.417	0.301	—	—	—	—	—	—	—	—	0.634	0.338	0.413	0.278	0.407	0.299	<u>0.396</u>	<u>0.275</u>	0.436	0.296
	720	<b>0.429</b>	<b>0.285</b>	0.453	0.314	—	—	—	—	—	—	—	—	0.640	0.351	0.449	0.299	0.438	0.310	<u>0.435</u>	<u>0.296</u>	0.466	0.315
	Avg	<b>0.386</b>	<b>0.261</b>	0.404	0.311	—	—	—	—	—	—	—	—	0.618	0.333	0.406	0.276	0.402	0.294	<u>0.394</u>	<u>0.274</u>	0.434	0.295
ECL	96	<b>0.130</b>	<u>0.225</u>	<u>0.132</u>	0.226	0.157	<b>0.211</b>	0.146	0.242	0.151	0.260	0.167	0.271	0.140	0.236	0.137	0.244	0.133	0.229	0.153	0.237		
	192	<b>0.148</b>	<b>0.242</b>	<u>0.151</u>	<u>0.244</u>	0.208	0.256	0.172	0.266	0.171	0.273	0.178	0.280	0.159	0.253	0.162	0.271	<u>0.151</u>	0.245	0.152	0.249		
	336	<b>0.164</b>	<b>0.259</b>	0.169	0.265	0.255	0.290	0.176	0.271	0.190	0.291	0.198	0.302	0.177	0.270	0.175	0.279	0.168	0.262	0.169	0.267		
	720	<u>0.203</u>	<b>0.293</b>	<b>0.201</b>	<b>0.291</b>	0.405	0.397	0.211	0.303	0.226	0.324	0.233	0.344	0.216	0.303	0.207	0.306	0.205	0.294	0.233	0.344		
	Avg	<b>0.161</b>	<b>0.255</b>	<u>0.163</u>	<u>0.257</u>	0.256	0.289	0.176	0.270	0.185	0.287	0.173	0.266	0.173	0.268	0.170	0.275	0.164	0.258	0.177	0.274		
Solar	96	<b>0.165</b>	<b>0.220</b>	0.177	0.235	—	—	0.197	0.244	0.202	<u>0.222</u>	—	—	—	0.179	<b>0.220</b>	0.224	0.289	0.183	0.265	0.191	0.256	
	192	<b>0.183</b>	<b>0.235</b>	<u>0.190</u>	0.249	—	—	0.230	0.274	0.216	0.240	—	—	—	0.198	<u>0.236</u>	0.244	0.289	0.205	0.283	0.211	0.273	
	336	<b>0.199</b>	<b>0.248</b>	<b>0.199</b>	0.262	—	—	0.244	0.281	0.236	0.255	—	—	—	<u>0.213</u>	<u>0.252</u>	0.225	0.291	0.224	0.299	0.228	0.287	
	720	0.219	0.266	<b>0.209</b>	0.276	—	—	0.247	0.280	0.252	<b>0.264</b>	—	—	—	0.239	0.277	0.243	0.301	0.239	0.316	0.236	0.295	
	Avg	<b>0.192</b>	<b>0.242</b>	0.194	<u>0.256</u>	—	—	0.230	0.270	0.227	0.276	—	—	—	0.207	0.246	0.234	0.293	0.213	0.291	0.217	0.278	

Table 1: The input length of the SE-LLM is 672. The forecast horizon is  $\{96, 192, 336, 720\}$ . The best results are in **bold** and the second best are underlined.

Models		SE-LLM	TimeMixer++ 2025	DECA 2025	Time-VLM 2025	AutoTimes 2024	S2IP-LLM 2024	Time-LLM 2024	FPT 2024	iTransformer 2024	Dlinear 2023	PatchTST 2023	TimesNet 2023
Yearly	SMAPE	<b>13.294</b>	13.397	13.288	13.419	<b>13.319</b>	13.413	13.419	15.531	13.652	14.012	13.517	13.394
	MASE	<b>2.970</b>	2.990	<u>2.974</u>	3.005	3.021	3.024	3.005	3.015	3.095	3.071	3.031	3.004
	OWA	<b>0.780</b>	0.786	<u>0.781</u>	0.789	0.789	0.792	0.789	0.793	0.807	0.815	0.795	0.787
Quarterly	SMAPE	10.079	10.206	10.037	10.110	<b>10.020</b>	10.352	10.110	10.177	10.353	10.758	10.847	10.101
	MASE	1.177	1.201	<u>1.174</u>	1.178	<b>1.162</b>	1.228	1.178	1.194	1.209	1.306	1.315	1.183
	OWA	0.887	0.901	<u>0.884</u>	0.889	<b>0.878</b>	0.922	0.889	0.897	0.911	0.905	0.972	0.890
Monthly	SMAPE	<b>12.618</b>	12.720	12.762	12.980	<b>12.696</b>	12.995	12.980	12.894	13.079	13.377	14.854	12.866
	MASE	<b>0.931</b>	0.943	0.947	0.963	<u>0.936</u>	0.970	0.963	0.956	0.974	1.021	1.169	0.964
	OWA	<b>0.875</b>	0.884	0.897	0.903	<b>0.880</b>	0.910	0.903	0.897	0.911	0.944	1.055	0.894
Others	SMAPE	4.896	<b>4.593</b>	<b>4.761</b>	4.795	4.916	4.805	4.795	4.940	4.780	5.259	6.184	4.892
	MASE	<b>3.306</b>	3.380	3.207	<u>3.178</u>	3.310	3.247	3.178	3.228	3.231	3.608	4.818	3.323
	OWA	1.037	1.054	<b>1.007</b>	1.006	1.039	1.017	1.006	1.029	1.012	1.122	1.140	1.048
Average	SMAPE	<b>11.778</b>	11.884	<u>11.828</u>	11.894	<b>11.831</b>	12.021	11.983	11.991	12.142	12.489	13.022	11.930
	MASE	<b>1.578</b>	1.597	<u>1.580</u>	1.592	<b>1.585</b>	1.612	1.595	1.600	1.631	1.690	1.814	1.597
	OWA	<b>0.847</b>	0.856	<u>0.850</u>	0.855	<b>0.850</b>	0.857	0.859	0.861	0.874	0.902	0.954	0.867

previously unencountered temporal patterns. We conducted zero-shot prediction experiments on the univariate datasets M3 and M4. Since most existing studies are not suitable for generalization on M3 and M4, we selected the SOTA methods listed in Table 3 for comparison. Specifically, the M3 and M4 datasets exhibit various temporal variation patterns with different data distributions. We discuss the domain generalization between these datasets. The results indicate that SE-LLM achieved the best performance in the zero-shot generalization comparison, further demonstrating its generalization capability. Compared to AutoTimes, the SMAPE decreased by 0.1% when transferring from M3 to M4, and by 1.4% when transferring from M4 to M3.

**In-Context Forecasting.** It was first introduced in AutoTimes (Liu et al. 2024b). Similar to AutoTime, we employ an autoregressive forecasting approach, enabling In-Context Forecasting. To rigorously evaluate SE-LLM’s performance, we conducted a comparative study against this baseline. The proposed approach shares conceptual similarities with zero-

shot prediction, wherein a model trained on source domain data  $\mathcal{D}_s$  is directly applied to target domains  $\mathcal{D}_t$  without re-training. The experimental results are shown in Fig. 5, indicating that we have achieved better performance.

### Ablation Study

**Ablation on Innovation Methods.** Ablation experiments are conducted on the ECL and Traffic datasets. To reduce computational costs, we selected different lightweight LLMs for comparison, including GPT2 (Radford et al. 2019), BERT (Devlin et al. 2019), Opt-125m (Zhang et al. 2022), and Qwen2.5-0.5B (Yang et al. 2024a), which are commonly used in current research (Zhou et al. 2023; Liu et al. 2024b, 2025; Jin et al. 2024). The experimental results are shown in Table 4. Our baseline uses a cross-domain attention mechanism for multi-modal alignment (Chang, Peng, and Chen 2025; Jin et al. 2024; Liu et al. 2025). After replacing it with the TSCC framework and adding the Time-Adapter, the prediction accuracy of different LLMs

Method	SE-LLM	AutoTimes	FPT	Dlinear	PatchTST	TimesNet	FEDformer	Informer	Reformer	
M3→M4	Yearly	<b>13.706</b>	<u>13.708</u>	13.740	14.193	13.966	15.655	13.887	18.542	15.662
	Quarterly	<b>10.718</b>	<u>10.742</u>	10.787	18.856	10.929	11.877	11.513	16.907	11.051
	Monthly	<b>14.553</b>	<u>14.558</u>	14.630	14.765	14.664	16.165	18.154	23.454	15.604
	Others	6.269	<b>6.259</b>	7.081	9.194	7.087	6.863	7.529	7.348	7.001
	Avg	<b>13.024</b>	<u>13.036</u>	13.125	15.337	13.228	14.553	15.047	19.047	14.092
M4→M3	Yearly	<b>13.692</b>	<u>15.731</u>	16.420	17.430	15.990	18.750	16.000	19.700	16.030
	Quarterly	<b>9.011</b>	<u>9.350</u>	10.130	9.740	9.620	12.260	9.480	13.000	9.760
	Monthly	<b>13.978</b>	<u>14.060</u>	14.100	15.650	14.710	<u>14.010</u>	15.120	15.910	14.800
	Others	4.872	5.790	<b>4.810</b>	6.810	9.440	6.880	8.940	13.030	7.530
	Avg	<b>12.560</b>	<u>12.750</u>	13.060	14.030	13.390	14.170	13.530	15.820	13.370

Table 3: The experimental results are based on the generalization of consistent temporal patterns. For non-matching patterns, we evaluate frequency transfers from Monthly to Weekly/Daily/Hourly in the M3 → M4 dataset, and from Quarterly to other frequencies in the M4 → M3 dataset.

has improved, demonstrating the effectiveness of the innovative methods in this paper. Comparative experiments show Qwen-0.5B yields lower prediction errors among LLMs.

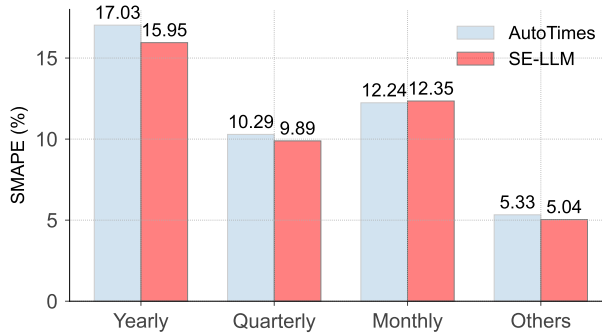


Figure 5: Results on M4 dataset. "Others" denotes the average values for weeks, days, and hours.

**Ablation on Adapters.** Long-term forecasting should capture long-term dependencies, making the task more challenging. Therefore, to demonstrate the performance of Time-Adapter, we conducted a comparison with the LoRA (Hu et al. 2022; Liu et al. 2024b), and the results are presented in Table 5. The experimental baseline is the Qwen2.5 with the TSCC module. Experiments findings clearly demonstrate that LoRA lacks generalization capability to enhance forecasting performance. In contrast, Time-Adapter endows LLM with the ability to adapt to forecasting tasks.

Datasets	Traffic		ECL		Solar		
	Metrics	MSE	MAE	MSE	MAE	MSE	MAE
Baseline: +TSCC	0.389	0.264	0.166	0.262	0.201	0.251	
+LoRA	0.390	0.268	0.163	0.257	0.202	0.253	
+Time-Adapter	<b>0.386</b>	<b>0.261</b>	<b>0.161</b>	<b>0.255</b>	<b>0.192</b>	<b>0.243</b>	

Table 5: All reported results are averaged. (Full results are in [Appendix](#))

**Ablation on LLM-based SOTA methods.** The modal disparity between time-series and language data is a chal-

lenging problem. To address this issue, we integrated the TSCC and the Time-Adapter as a plugin into the Time-LLM (Jin et al. 2024), AutoTimes (Liu et al. 2024b), and TimeCMA (Liu et al. 2025). We analyzed their impact on algorithm performance using the ETTh and ETThm datasets. Our experiments were conducted based on the parameters provided in the source code. All other experimental parameters remained unchanged when incorporating the TSCC and Time-Adapter, with the GPT-2 model consistently used as the LLM. The experimental results, listed in Table 6, indicate that errors were reduced across the board. However, Time-LLM yielded negligible performance improvements on the ETThm dataset. Notably, for the TimeCMA model, the Mean Squared Error (MSE) reduces significantly. Specifically, on the ETTh2 dataset, the MSE was reduced by 8.9%. TimeCMA uses large language models as the output of time-series text prompts. The LLM does not participate in the training, making conducting ablation experiments on Time-Adapter impossible. The experiment results highlight that our research addresses a common issue in existing studies.

	Datasets	ETTh1		ETTh2		ETThm1		ETThm2	
		MSE	MAE	MSE	MAE	MSE	MAE	MSE	MAE
Time-LLM	Baseline	0.420	0.439	0.370	0.404	0.358	0.389	<b>0.262</b>	<b>0.324</b>
	TSCC	0.407	0.429	0.368	0.401	0.360	0.390	0.267	0.328
	Time-Adapter	<b>0.405</b>	<b>0.428</b>	<b>0.364</b>	<b>0.399</b>	<b>0.357</b>	<b>0.388</b>	0.266	0.326
AutoTimes	Baseline	0.397	0.425	0.367	0.410	0.361	0.389	0.274	0.329
	TSCC	0.390	0.421	0.363	<b>0.406</b>	0.354	0.384	0.269	0.325
	Time-Adapter	<b>0.388</b>	<b>0.420</b>	0.357	<b>0.407</b>	<b>0.351</b>	<b>0.382</b>	<b>0.268</b>	<b>0.323</b>
Time-CMA	Baseline	0.446	0.446	0.416	0.429	0.399	0.413	0.294	0.337
	TSCC	0.437	0.434	0.379	<b>0.403</b>	<b>0.383</b>	<b>0.396</b>	<b>0.285</b>	<b>0.322</b>

Table 6: The forecasting horizons are in {96, 192, 336, 720}, and all experimental results presented are averages. (Full results are in [Appendix](#))

## Qualitative Analysis

In this section, we conduct a qualitative analysis of how TSCC injects temporal patterns into the joint space. Fig. 6 (a) presents the visualization results of the semantic space, while Fig. 6 (b) displays the learned time series embeddings. Fig. 6 (c) shows the extracted results of anomaly parts in the joint space. The TSCC module accurately reveals distinct

LLM	GPT2				Bert				Opt125m				Qwen2.5-0.5B			
Dataset	ELC		Traffic		ELC		Traffic		ELC		Traffic		ELC		Traffic	
Metric	MSE	MAE	MSE	MAE	MSE	MAE	MSE	MAE	MSE	MAE	MSE	MAE	MSE	MAE	MSE	MAE
Baseline	0.145	0.240	0.387	0.267	0.150	0.245	0.440	0.304	0.140	0.237	0.368	0.258	0.135	0.233	0.373	0.263
	0.165	0.257	0.410	0.277	0.168	0.262	0.459	0.314	0.158	0.254	0.390	0.268	0.152	0.249	0.394	0.272
	0.183	0.275	0.427	0.286	0.187	0.281	0.476	0.322	0.176	0.272	0.407	0.292	0.170	0.267	0.409	0.280
	0.224	0.309	0.463	0.306	0.230	0.316	0.514	0.344	0.216	0.305	0.445	0.300	0.212	0.303	0.444	0.300
+TSCC	0.179	0.270	0.422	0.284	0.184	0.276	0.472	0.321	0.173	0.267	0.403	0.280	0.167	0.263	0.405	0.279
	0.138	0.233	0.368	0.257	0.144	0.240	0.395	0.277	0.136	0.232	0.361	0.251	0.134	0.231	0.356	0.247
	0.157	0.250	0.393	0.269	0.161	0.256	0.417	0.286	0.154	0.249	0.383	0.263	0.152	0.248	0.377	0.257
	0.176	0.269	0.414	0.281	0.181	0.274	0.436	0.295	0.173	0.267	0.401	0.271	0.169	0.266	0.393	0.266
+Time-Adapter	0.218	0.305	0.461	0.312	0.223	0.309	0.474	0.316	0.215	0.303	0.439	0.294	0.210	0.301	0.431	0.287
	0.172	0.264	0.409	0.280	0.177	0.270	0.431	0.294	0.170	0.263	0.396	0.270	0.166	0.262	0.389	0.264
	0.133	0.227	0.363	0.255	0.135	0.230	0.378	0.266	0.132	0.227	0.354	0.247	0.130	0.225	0.350	0.243
	0.152	0.244	0.388	0.267	0.152	0.247	0.400	0.275	0.149	0.243	0.378	0.258	0.148	0.242	0.373	0.254
+Time-Adapter	0.169	0.262	0.411	0.281	0.170	0.265	0.417	0.283	0.166	0.261	0.396	0.267	0.164	0.259	0.390	0.263
	0.211	0.299	0.461	0.314	0.209	0.298	0.454	0.303	0.204	0.295	0.434	0.291	0.203	0.293	0.429	0.285
	0.166	0.258	0.406	0.279	0.167	0.260	0.412	0.282	0.163	0.257	0.391	0.266	0.161	0.255	0.386	0.261

Table 4: In the ablation experiments, we set the input length to 672 and the output length to 96, with forecast lengths from the set {96, 192, 336, 720}.

clustering characteristics in the data exhibiting anomaly patterns. This indicates that through the TSCC module, we can obtain enhanced semantics with temporal patterns that are more distinguishable.

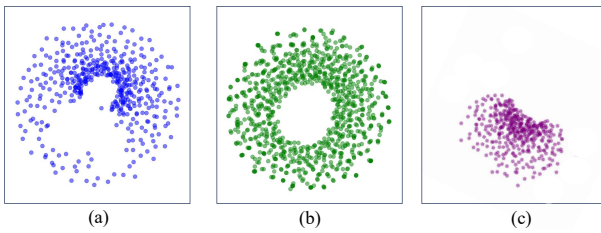


Figure 6: The t-SNE plots of embeddings space

## Computational Efficiency

From the perspectives of computational efficiency and prediction error, the results in Fig. 7 indicate that Qwen2.5-0.5B offers relatively lower computational consumption with lower errors on the ECL dataset, making it more suitable for long-term forecasting in SE-LLM.

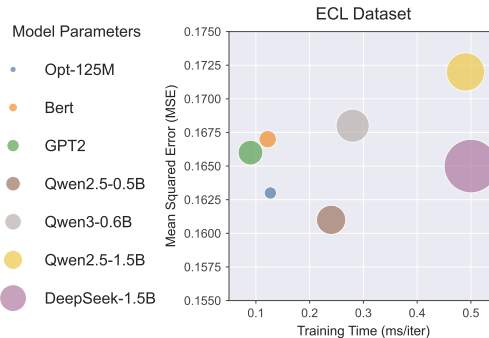


Figure 7: The size of the circles reflects the proportional relationship among the parameter counts of different LLMs

Compared to current research, we selected two representative studies, AutoTimes and Time-LLM. First, we compared the performance under their respective optimal prediction conditions. Then, we further evaluated their computational efficiency, including training and inference time. Referring to the results in Fig. 8, our method achieves improved performance.

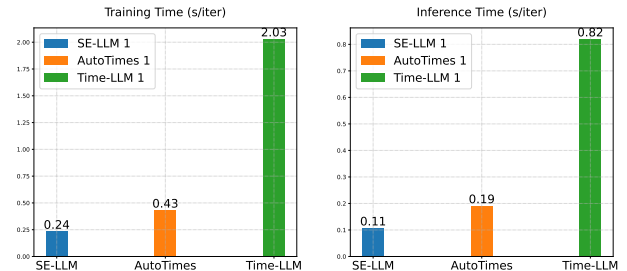


Figure 8: All experiments use a batch size of 256.

## Conclusion

This paper introduces SE-LLM, which addresses the inherent modality gap between LLMs and time series data. We explore the temporal and channel dependencies between temporal embeddings and the semantic space of LLMs. Token embeddings are enhanced with temporal-pattern semantic information, improving interpretability and unlocking LLMs' potential. Moreover, we incorporate a plugin module tailored for time-series forecasting into LLMs, which activates their ability to model temporal dependencies. Experimental results demonstrate that SE-LLM surpasses SOTA performance. Furthermore, embedding TSCC and Time-Adapter into existing frameworks also leads to performance improvements, shedding light on common challenges in leveraging LLMs for time-series forecasting. SE-LLM efficiently integrates temporal information and language models.

## References

Arslan, S. 2022. A hybrid forecasting model using LSTM and Prophet for energy consumption with decomposition of time series data. *PeerJ Computer Science*, 8: 1001.

Cao, D.; Wang, Y.; Duan, J.; and *et al.* 2020. Spectral temporal graph neural network for multivariate time-series forecasting. *Advances in neural information processing systems*, 33: 17766–17778.

Cemgil, T.; Ghaisas, S.; Dvijotham, K.; and *et al.* 2020. The autoencoding variational autoencoder. *Advances in Neural Information Processing Systems*, 33: 15077–15087.

Chang, C.; Peng, W.; and Chen, T. 2025. LLM4TS: Two-Stage Fine-Tuning for Time-Series Forecasting with Pre-Trained LLMs. In *ACM Transactions on Intelligent Systems and Technology*, 1–20.

Chen, C.; Oliveira, G. L.; Sharifi-Noghabi, H.; and *et al.* 2025. LLM-TS Integrator: Integrating LLM for Enhanced Time Series Modeling. *Trans. Mach. Learn. Res.*, 2025.

Chen, M.; Peng, H.; Fu, J.; and *et al.* 2021. AutoFormer: Searching Transformers for Visual Recognition. In *International Conference on Computer Vision*, 12250–12260.

Chen, S.; Jie, Z.; and Ma, L. 2024. LLaVA-MoLE: Sparse Mixture of LoRA Experts for Mitigating Data Conflicts in Instruction Finetuning MLLMs. *CoRR*, abs/2401.16160.

DeepSeek-AI; Liu, A.; Feng, B.; and *et al.* 2024. DeepSeek-V2: A Strong, Economical, and Efficient Mixture-of-Experts Language Model. *CoRR*, abs/2405.04434.

Deng, S.; Wang, S.; Rangwala, H.; and *et al.* 2020. Cola-GNN: Cross-location attention based graph neural networks for long-term ILI prediction. In *ACM international conference on information & knowledge management*, 245–254.

Devlin, J.; Chang, M.; Lee, K.; and *et al.* 2019. BERT: Pre-training of Deep Bidirectional Transformers for Language Understanding. In *North American Chapter of the Association for Computational Linguistics*, 4171–4186.

Du, C.; Li, Y.; Qiu, Z.; and Xu, C. 2023. Stable diffusion is unstable. *Advances in Neural Information Processing Systems*, 36: 58648–58669.

Fang, Z.; Zhu, X.; Yang, C.; Han, Z.; Qin, J.; and Yin, X.-C. 2022. Learning aligned cross-modal representation for generalized zero-shot classification. In *Proceedings of the AAAI conference on artificial intelligence*, volume 36, 6605–6613.

Fang, Z.; Zhu, X.; Yang, C.; Zhou, H.; Qin, J.; and Yin, X.-C. 2025. Aligning enhanced feature representation for generalized zero-shot learning. *Science China Information Sciences*, 68(2): 122102.

Gruver, N.; Finzi, M.; Qiu, S.; and *et al.* 2023. Large language models are zero-shot time series forecasters. *Advances in Neural Information Processing Systems*, 36: 19622–19635.

Guo, H.; Greengard, P.; Xing, E. P.; and *et al.* 2024. LQ-LoRA: Low-rank plus Quantized Matrix Decomposition for Efficient Language Model Finetuning. In *International Conference on Learning Representations*.

Gupta, D.; Bhatti, A.; Parmar, S.; and *et al.* 2024. Low-rank adaptation of time series foundational models for out-of-domain modality forecasting. In *International Conference on Multimodal Interaction*, 382–386.

Hochreiter, S.; and Schmidhuber, J. 1997. Long short-term memory. *Neural computation*, 9: 1735–1780.

Hu, E. J.; Shen, Y.; Wallis, P.; and *et al.* 2022. Lora: Low-rank adaptation of large language models. *International Conference on Machine Learning*, 1(2): 3.

Hu, Y.; Li, Q.; Zhang, D.; and *et al.* 2025. Context-Alignment: Activating and Enhancing LLM Capabilities in Time Series. *CoRR*, abs/2501.03747.

Jia, F.; Wang, K.; Zheng, Y.; and *et al.* 2024a. Gpt4mts: Prompt-based large language model for multimodal time-series forecasting. In *AAAI Conference on Artificial Intelligence*, volume 38, 23343–23351.

Jia, Y.; Lin, Y.; Yu, J.; and *et al.* 2024b. PGN: The RNN’s New Successor is Effective for Long-Range Time Series Forecasting. *Advances in Neural Information Processing Systems*, 37: 84139–84168.

Jin, M.; Wang, S.; Ma, L.; and *et al.* 2024. Time-LLM: Time Series Forecasting by Reprogramming Large Language Models. In *International Conference on Learning Representations*.

Khaldi, R.; El Afia, A.; Chiheb, R.; and *et al.* 2023. What is the best RNN-cell structure to forecast each time series behavior? *Expert Systems with Applications*, 215: 119140.

Kitaev, N.; Kaiser, L.; and Levskaya, A. 2020. Reformer: The Efficient Transformer. In *International Conference on Learning Representations*.

Kong, Y.; Wang, Z.; Nie, Y.; and *et al.* 2025. Unlocking the power of lstm for long term time series forecasting. In *AAAI Conference on Artificial Intelligence*, volume 39, 11968–11976.

Lai, G.; Chang, W.; Yang, Y.; and *et al.* 2018. Modeling Long- and Short-Term Temporal Patterns with Deep Neural Networks. In *Research & Development in Information Retrieval*, 95–104.

Lester, B.; Al-Rfou, R.; and Constant, N. 2021. The Power of Scale for Parameter-Efficient Prompt Tuning. In *Empirical Methods in Natural Language Processing*, 3045–3059.

Lin, S.; Lin, W.; Hu, X.; and *et al.* 2024. Cyclenet: enhancing time series forecasting through modeling periodic patterns. *Advances in Neural Information Processing Systems*, 37: 106315–106345.

Liu, C.; Hoi, S. C. H.; Zhao, P.; and *et al.* 2016. Online ARIMA Algorithms for Time Series Prediction. In *AAAI Conference on Artificial Intelligence*, 1867–1873.

Liu, C.; Xu, Q.; Miao, H.; and *et al.* 2025. TimeCMA: Towards LLM-Empowered Multivariate Time Series Forecasting via Cross-Modality Alignment. In *AAAI Conference on Artificial Intelligence*, 18780–18788.

Liu, S.; Zeng, Z.; and Ren, T. t. 2024. Grounding dino: Marrying dino with grounded pre-training for open-set object detection. In *European Conference on Computer Vision*, 38–55. Springer.

Liu, Y.; Hu, T.; Zhang, H.; and *et al.* 2024a. iTransformer: Inverted Transformers Are Effective for Time Series Forecasting. In *International Conference on Learning Representations*.

Liu, Y.; Li, C.; Wang, J.; and Long, M. 2023. Koopa: Learning non-stationary time series dynamics with koopman predictors. *Advances in neural information processing systems*, 36: 12271–12290.

Liu, Y.; Qin, G.; Huang, X.; and *et al.* 2024b. Autotimes: Autoregressive time series forecasters via large language models. *Advances in Neural Information Processing Systems*, 37: 122154–122184.

Ma, S.; Zhang, T.; Zhao, Y.-B.; Kang, Y.; and Bai, P. 2023. TCLN: A Transformer-based Conv-LSTM network for multivariate time series forecasting. *Applied Intelligence*, 53(23): 28401–28417.

Makridakis, S.; Spiliotis, E.; and Assimakopoulos, V. 2020. The M4 Competition: 100,000 time series and 61 forecasting methods. *International Journal of Forecasting*, 36(1): 54–74.

Mu, J.; Wang, W.; Liu, W.; and *et al.* 2024. Multimodal Large Language Model with LoRA Fine-Tuning for Multimodal Sentiment Analysis. *ACM Transactions on Intelligent Systems and Technology*.

Nie, Y.; Nguyen, N. H.; Sinthong, P.; and *et al.* 2023. A Time Series is Worth 64 Words: Long-term Forecasting with Transformers. In *International Conference on Learning Representations*.

Pan, Z.; Jiang, Y.; Garg, S.; and *et al.* 2024a. S2IP-LLM: Semantic Space Informed Prompt Learning with LLM for Time Series Forecasting. In *International Conference on Machine Learning*.

Pan, Z.; Jiang, Y.; Song, D.; and *et al.* 2024b. Structural Knowledge Informed Continual Multivariate Time Series Forecasting. *CoRR*, abs/2402.12722.

Qin, Y.; Song, D.; Chen, H.; and *et al.* 2017. A Dual-Stage Attention-Based Recurrent Neural Network for Time Series Prediction. In *International Joint Conference on Artificial Intelligence*, 2627–2633.

Radford, A.; Wu, J.; Child, R.; and *et al.* 2019. Language models are unsupervised multitask learners. *OpenAI blog*, 1(8): 9.

Shang, Z.; Chen, L.; Wu, B.; and *et al.* 2024. Ada-MSHyper: adaptive multi-scale hypergraph transformer for time series forecasting. *Advances in Neural Information Processing Systems*, 37: 33310–33337.

Sherstinsky, A. 2020. Fundamentals of recurrent neural network (RNN) and long short-term memory (LSTM) network. *Physica D: Nonlinear Phenomena*, 404: 132306.

Shi, X.; Wang, S.; Nie, Y.; and *et al.* 2025. Time-MoE: Billion-Scale Time Series Foundation Models with Mixture of Experts. In *International Conference on Learning Representations*.

Touvron, H.; Lavril, T.; Izacard, G.; and *et al.* 2023. LLaMA: Open and Efficient Foundation Language Models. *CoRR*, abs/2302.13971.

Wang, H.; Mo, Y.; Xiang, K.; and *et al.* 2025a. CSformer: Combining Channel Independence and Mixing for Robust Multivariate Time Series Forecasting. In *Association for the Advancement of Artificial Intelligence*, 21090–21098.

Wang, S.; Li, J.; Shi, X.; and *et al.* 2025b. TimeMixer++: A General Time Series Pattern Machine for Universal Predictive Analysis. In *International Conference on Learning Representations*.

Wang, Y.; Wu, H.; Dong, J.; Qin, G.; and *et al.* 2024. TimeXer: Empowering Transformers for Time Series Forecasting with Exogenous Variables. In *Advances in Neural Information Processing Systems*.

Wu, H.; Hu, T.; Liu, Y.; and *et al.* 2023. TimesNet: Temporal 2D-Variation Modeling for General Time Series Analysis. In *International Conference on Learning Representations*.

Xue, H.; and Salim, F. D. 2023. Promptcast: A new prompt-based learning paradigm for time series forecasting. *IEEE Transactions on Knowledge and Data Engineering*, 36(11): 6851–6864.

Yang, A.; Zhang, B.; Hui, B.; and *et al.* 2024a. Qwen2.5-Math Technical Report: Toward Mathematical Expert Model via Self-Improvement. *CoRR*, abs/2409.12122.

Yang, R.; Cao, L.; Yang, J.; and *et al.* 2024b. Rethinking Fourier Transform from A Basis Functions Perspective for Long-term Time Series Forecasting. In *Advances in Neural Information Processing Systems*.

Yeo, K.; Melnyk, I.; Nguyen, N.; and *et al.* 2018. DERNN: Forecasting the probability density function of non-linear time series. In *IEEE international conference on data mining*, 697–706.

Zaheer, S.; Anjum, N.; Hussain, S.; and *et al.* 2023. A multi parameter forecasting for stock time series data using LSTM and deep learning model. *Mathematics*, 11: 590.

Zeng, A.; Chen, M.; Zhang, L.; and *et al.* 2023. Are transformers effective for time series forecasting? In *AAAI conference on artificial intelligence*, volume 37, 11121–11128.

Zhang, J.; Zhu, W.; and Gao, J. 2025. Adapting Large Language Models for Time Series Modeling via a Novel Parameter-efficient Adaptation Method. *CoRR*, abs/2502.13725.

Zhang, L.; Zhang, L.; Shi, S.; and *et al.* 2023. LoRA-FA: Memory-efficient Low-rank Adaptation for Large Language Models Fine-tuning. *CoRR*, abs/2308.03303.

Zhang, S.; Roller, S.; Goyal, N.; and *et al.* 2022. OPT: Open Pre-trained Transformer Language Models. *CoRR*, abs/2205.01068.

Zhang, Y.; and Yan, J. 2023. Crossformer: Transformer Utilizing Cross-Dimension Dependency for Multivariate Time Series Forecasting. In *International Conference on Learning Representations*.

Zhong, S.; Ruan, W.; Jin, M.; and *et al.* 2025. Time-VLM: Exploring Multimodal Vision-Language Models for Augmented Time Series Forecasting. *CoRR*, abs/2502.04395.

Zhou, H.; Zhang, S.; Peng, J.; and *et al.* 2021. Informer: Beyond efficient transformer for long sequence time-series

forecasting. In *AAAI conference on artificial intelligence*, volume 35, 11106–11115.

Zhou, T.; Niu, P.; Sun, L.; and *et al.* 2023. One fits all: Power general time series analysis by pretrained lm. *Advances in neural information processing systems*, 36: 43322–43355.

## Appendix

### Autoregressive Forecasting

In time series forecasting, the autoregressive model can accomplish predictions for any time step length by merely training on data with a fixed step length, significantly reducing computational costs.

Autoregressive models generate future predictions by iteratively conditioning on historical observations. This strictly sequential prediction strategy relies on the temporal continuity and internal patterns embedded in past data. When such patterns remain consistent over time, autoregressive approaches typically yield stable and reliable forecasts.

SE-LLM adopts an autoregressive inference scheme, inspired by the design of AutoTimes. Specifically, we generate future values by recursively feeding the model’s previous outputs into the input sequence. The complete procedure is outlined in Algorithm 2.

---

#### Algorithm 2: Gated Attention Prediction Procedure

---

**Require:** Input time series  $\mathbf{X} \in \mathbb{R}^{B \times L}$ , where  $B$  is the batch size and  $L$  is the sequence length. Output sequence  $\mathbf{Y} \in \mathbb{R}^{B \times T}$ .

```

1: if  $N = T \text{ div } \tau$  then
2:   for  $\text{id} \leftarrow 1$  to  $N$  do
3:      $\hat{\mathbf{Y}} \leftarrow \text{Model}(\mathbf{X})$ 
4:      $\hat{\mathbf{X}} \leftarrow \text{Cat}(\mathbf{X}_{\tau:L}, \hat{\mathbf{Y}}_{L-\tau:L})$ 
5:   end for
6:   return  $\hat{\mathbf{X}}$ 
7: end if
8:  $l \leftarrow T \bmod \tau$ 
9: for  $\text{id} \leftarrow 1$  to  $(N + 1)$  do
10:   $\hat{\mathbf{Y}} \leftarrow \text{Model}(\mathbf{X})$ 
11:   $\hat{\mathbf{X}} \leftarrow \text{Cat}(\mathbf{X}_{\tau:L}, \hat{\mathbf{Y}}_{L-\tau:L})$ 
12:  if  $\text{id} = N + 1$  then
13:     $\hat{\mathbf{X}} \leftarrow \text{Cat}(\mathbf{X}_{\tau:L}, \hat{\mathbf{Y}}_{L-\tau+l:L})$ 
14:  return  $\hat{\mathbf{X}}$ 
15:  end if
16: end for
17: return  $\hat{\mathbf{X}}$ 

```

---

### Evaluation Metrics

In time series forecasting, quantitative evaluation is essential for assessing model performance. In this study, we adopt standard metrics tailored to different forecasting scenarios. For long-term forecasting, we use Mean Squared Error (MSE) and Mean Absolute Error (MAE):

$$\text{MAE} = \frac{1}{N} \sum_{n=1}^N |\mathbf{Y}_n - \hat{\mathbf{Y}}_n|, \quad (10)$$

$$\text{MSE} = \frac{1}{N} \sum_{n=1}^N (\mathbf{Y}_n - \hat{\mathbf{Y}}_n)^2. \quad (11)$$

MAE reflects the average magnitude of forecast errors, while MSE penalizes larger deviations more heavily due to the squaring operation. For short-term and zero-shot forecasting on the M4 and M3 dataset, we additionally employ the following metrics:

Mean Absolute Percentage Error (MAPE):

$$\text{MAPE} = \frac{100}{N} \sum_{n=1}^N \frac{|\mathbf{Y}_n - \hat{\mathbf{Y}}_n|}{|\mathbf{Y}_n|}, \quad (12)$$

Symmetric Mean Absolute Percentage Error (SMAPE):

$$\text{SMAPE} = \frac{200}{N} \sum_{n=1}^N \frac{|\mathbf{Y}_n - \hat{\mathbf{Y}}_n|}{|\mathbf{Y}_n| + |\hat{\mathbf{Y}}_n|}, \quad (13)$$

Mean Absolute Scaled Error (MASE):

$$\text{MASE} = \frac{1}{N} \sum_{n=1}^N \frac{|\mathbf{Y}_n - \hat{\mathbf{Y}}_n|}{\frac{1}{N-m} \sum_{j=m}^N |\mathbf{Y}_j - \mathbf{Y}_{j-m}|}, \quad (14)$$

Overall Weighted Average (OWA):

$$\text{OWA} = \frac{1}{2} \left( \frac{\text{SMAPE}}{\text{SMAPE}_{\text{Naive2}}} + \frac{\text{MASE}}{\text{MASE}_{\text{Naive2}}} \right). \quad (15)$$

MAPE and SMAPE provide scale-invariant percentage-based error assessments, with SMAPE mitigating issues related to small denominators. MASE offers a relative comparison against a naive seasonal benchmark. OWA combines MASE and SMAPE relative to the Naive2 baseline, serving as a composite indicator of overall performance.

### Datasets

Time series datasets consist of sequential data points collected or recorded at consistent time intervals (e.g., hourly, daily, monthly). Each entry includes a timestamp and one or more observed values. These datasets are used to train models that identify historical patterns to forecast future values. Common applications include predicting stock prices, energy demand, weather, sales, and website traffic. The detailed content are shown in Table 7.

### Full Experiment Results

**Ablation on Adapters.** Full results are shown in Table 8.

**Ablation on LLM-based SOTA methods.** Full results are shown in Table 9.

### Show Case

The visualization results for long-term forecasting are illustrated in Figure 9, where we selected examples featuring periodic patterns and abrupt anomaly mutations to demonstrate how the innovative method activates the predictive capabilities of LLMs. It is noteworthy that, in the prediction results for a 96-step horizon on the Weather dataset, we have accurately modeled abnormal sudden changes based on historical data. This demonstrates the effectiveness of the TSCC module in modeling anomaly patterns.

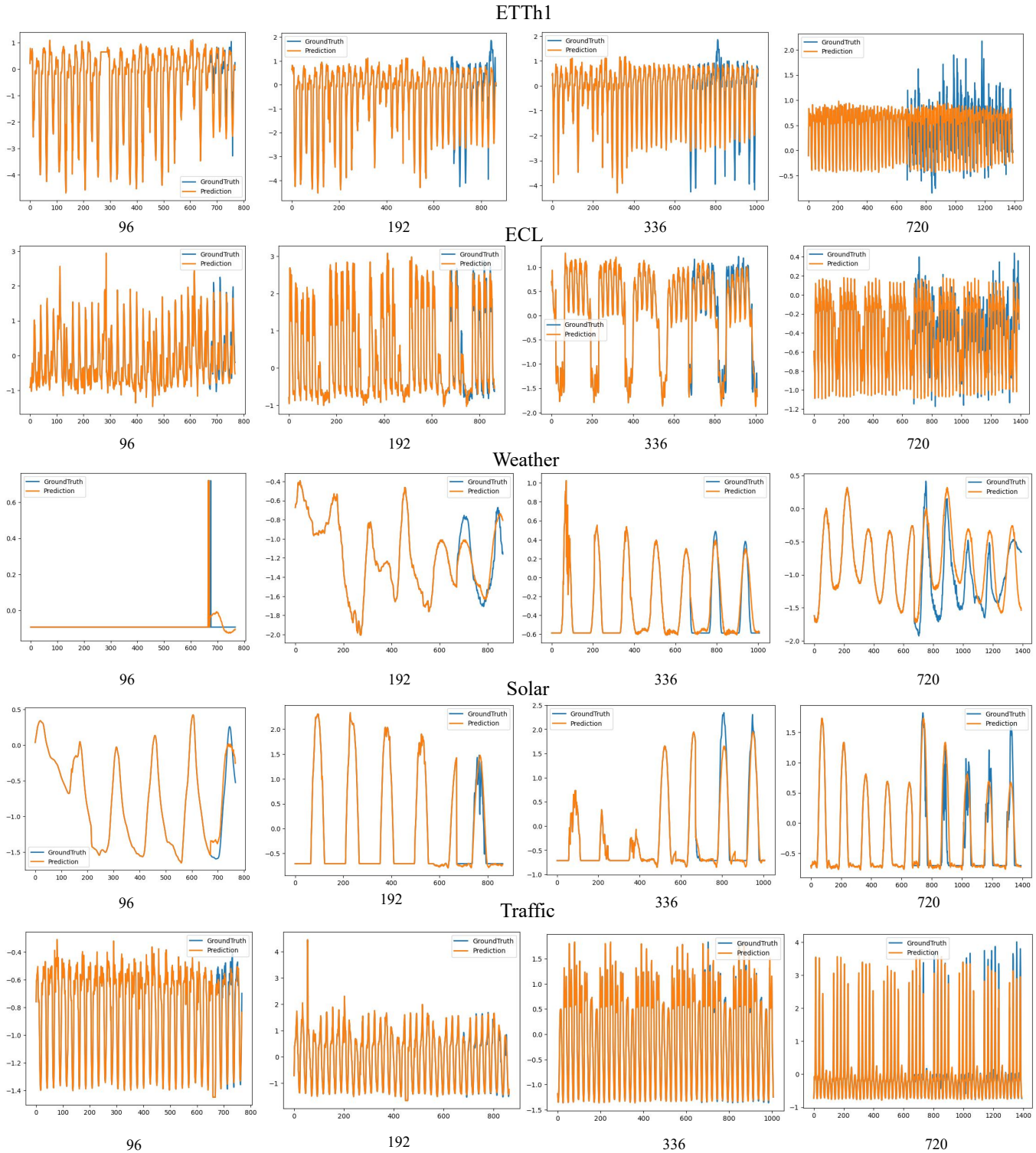


Figure 9: Visualization of Long-Term Prediction

Tasks	Datasets	Dim	Series Length	Dataset Size	Frequency	Information
Long-Term Forecasting	ETTh1	7	{96, 192, 336, 720}	{8545, 2881, 2881}	Hourly	Electricity
	Weather	21	{96, 192, 336, 720}	{36792, 5271, 10540}	10min	Weather
	Traffic	862	{96, 192, 336, 720}	{12185, 1757, 3509}	Hourly	Transportation
	ECL	321	{96, 192, 336, 720}	{18317, 2633, 5261}	Hourly	Electricity
	Solar	137	{96, 192, 336, 720}	{36601, 5161, 10417}	10min	Energy
Short-Term Forecasting and Zero-Shot Forecasting	M4-Yearly	1	6	{23000, 0, 23000}	Yearly	Demographic
	M4-Quarterly	1	8	{24000, 0, 24000}	Quarterly	Finace
	M4-Monthly	1	18	{48000, 0, 48000}	Monthly	Industry
	M4-Weekly	1	13	{359, 0, 359}	Weekly	Macro
	M4-Daily	1	14	{4227, 0, 4227}	Daily	Macro
	M4-Hourly	1	48	{414, 0, 414}	Hourly	Other
Zero-Shot Forecasting	M3-Yearly	1	6	{645, 0, 645}	Yearly	Demographic
	M3-Quarterly	1	8	{756, 0, 756}	Quarterly	Finace
	M3-Monthly	1	18	{1428, 0, 1428}	Monthly	Industry
	M3-Others	1	8	{174, 0, 174}	Others	Macro

Table 7: The dataset includes detailed descriptions, with specifications such as dimensionality, the distribution of total time points across training, validation, and test partitions, the target range of future time points for prediction, and the temporal sampling rate.

Datasets	ETTh1		Weather		Traffic		ECL		Solar	
Metrics	MSE	MAE								
TSCC	<b>0.352</b>	<b>0.393</b>	0.162	0.245	<b>0.356</b>	<b>0.247</b>	0.134	0.231	0.175	0.230
	<b>0.378</b>	<b>0.411</b>	0.209	0.259	<b>0.377</b>	<b>0.257</b>	0.152	0.248	<b>0.194</b>	<b>0.245</b>
	<b>0.391</b>	<b>0.420</b>	0.263	0.299	<b>0.393</b>	<b>0.266</b>	0.169	0.266	<b>0.209</b>	<b>0.257</b>
	<b>0.402</b>	<b>0.437</b>	<b>0.332</b>	<b>0.346</b>	0.431	<b>0.287</b>	0.210	0.301	<b>0.227</b>	<b>0.270</b>
	<b>0.381</b>	<b>0.415</b>	0.242	0.287	0.389	<b>0.264</b>	0.166	0.262	<b>0.201</b>	<b>0.251</b>
+LoRA	0.362	0.399	<b>0.157</b>	<b>0.210</b>	0.357	0.251	<b>0.132</b>	<b>0.228</b>	<b>0.173</b>	0.228
	0.393	<b>0.420</b>	<b>0.204</b>	<b>0.254</b>	0.378	0.260	<b>0.149</b>	<b>0.244</b>	<b>0.194</b>	<b>0.245</b>
	0.410	<b>0.432</b>	<b>0.260</b>	<b>0.297</b>	0.394	0.269	<b>0.166</b>	<b>0.261</b>	0.210	0.260
	0.418	<b>0.447</b>	0.339	0.351	0.430	0.290	<b>0.205</b>	<b>0.295</b>	0.229	0.277
	0.396	<b>0.425</b>	0.240	0.278	0.390	0.268	0.163	0.257	0.202	0.253
+Time-Adapter	<b>0.355</b>	<b>0.398</b>	<b>0.150</b>	<b>0.200</b>	<b>0.350</b>	<b>0.243</b>	<b>0.130</b>	<b>0.225</b>	<b>0.165</b>	<b>0.220</b>
	<b>0.389</b>	0.421	<b>0.194</b>	<b>0.243</b>	<b>0.373</b>	<b>0.254</b>	<b>0.148</b>	<b>0.242</b>	<b>0.183</b>	<b>0.236</b>
	<b>0.409</b>	0.435	<b>0.247</b>	<b>0.285</b>	<b>0.390</b>	<b>0.263</b>	<b>0.164</b>	<b>0.259</b>	<b>0.199</b>	<b>0.249</b>
	<b>0.418</b>	0.448	<b>0.323</b>	<b>0.339</b>	<b>0.429</b>	<b>0.285</b>	<b>0.203</b>	<b>0.293</b>	<b>0.219</b>	<b>0.266</b>
	<b>0.393</b>	0.426	<b>0.229</b>	<b>0.267</b>	<b>0.386</b>	<b>0.261</b>	<b>0.161</b>	<b>0.255</b>	<b>0.192</b>	<b>0.243</b>

Table 8: Time-Adapter compared with LoRA. The forecasting horizons were set to {96, 192, 336, 720}.

		Time-LLM							
		ETTh1		ETTh2		ETTm1		ETTm2	
		MSE	MAE	MSE	MAE	MSE	MAE	MSE	MAE
Baseline	0.384	0.411	0.293	0.349	<b>0.300</b>	0.356	<b>0.172</b>	<b>0.265</b>	
	0.414	0.430	0.379	0.400	<b>0.340</b>	0.378	<b>0.232</b>	<b>0.306</b>	
	0.433	0.448	<b>0.381</b>	0.414	0.370	<b>0.395</b>	<b>0.281</b>	<b>0.339</b>	
	0.448	0.468	0.428	0.452	<b>0.422</b>	0.428	<b>0.362</b>	<b>0.387</b>	
	0.420	0.439	0.370	0.404	<b>0.358</b>	0.389	<b>0.262</b>	<b>0.324</b>	
TSCC	<u>0.373</u>	<u>0.401</u>	<b>0.287</b>	<u>0.352</u>	<u>0.302</u>	<b>0.354</b>	0.180	0.270	
	<u>0.403</u>	<u>0.425</u>	<b>0.367</b>	<b>0.393</b>	<u>0.341</u>	0.378	0.247	0.314	
	<u>0.414</u>	<u>0.430</u>	0.390	<u>0.414</u>	<u>0.373</u>	0.399	<u>0.276</u>	<u>0.335</u>	
	<u>0.436</u>	<u>0.460</u>	0.426	<u>0.446</u>	<u>0.422</u>	<b>0.427</b>	0.366	0.391	
	<u>0.407</u>	<u>0.429</u>	0.368	<u>0.401</u>	0.360	0.390	0.267	0.328	
Time-Adapter	<b>0.368</b>	<b>0.400</b>	0.294	<u>0.347</u>	0.303	<b>0.354</b>	<u>0.178</u>	<u>0.268</u>	
	<b>0.401</b>	<b>0.421</b>	<u>0.370</u>	<u>0.400</u>	0.345	<b>0.376</b>	<b>0.229</b>	<b>0.303</b>	
	<b>0.412</b>	<b>0.430</b>	<u>0.373</u>	<b>0.402</b>	<b>0.366</b>	<u>0.394</u>	0.291	0.342	
	<b>0.439</b>	<b>0.459</b>	<u>0.418</u>	<u>0.445</u>	<u>0.414</u>	<u>0.428</u>	<u>0.364</u>	<u>0.391</u>	
	<b>0.405</b>	<b>0.428</b>	<u>0.364</u>	<u>0.399</u>	<u>0.357</u>	<u>0.388</u>	<u>0.266</u>	<u>0.326</u>	
		AutoTimes							
		ETTh1		ETTh2		ETTm1		ETTm2	
		MSE	MAE	MSE	MAE	MSE	MAE	MSE	MAE
Baseline	0.360	0.397	0.288	0.352	0.291	0.347	0.176	0.264	
	0.391	0.419	0.351	0.395	0.338	0.376	0.238	0.307	
	0.408	0.432	0.383	0.424	0.376	0.398	0.298	0.346	
	0.429	0.452	0.447	0.468	0.438	0.433	0.382	0.400	
	0.397	0.425	0.367	0.410	0.361	0.389	0.274	0.329	
TSCC	<u>0.354</u>	<u>0.394</u>	<u>0.288</u>	<u>0.352</u>	<u>0.286</u>	<u>0.341</u>	<u>0.174</u>	<u>0.261</u>	
	<u>0.385</u>	<u>0.415</u>	<u>0.350</u>	<u>0.393</u>	<u>0.334</u>	<u>0.371</u>	<u>0.236</u>	<u>0.303</u>	
	<u>0.401</u>	<u>0.427</u>	<u>0.378</u>	<u>0.419</u>	<u>0.370</u>	<u>0.394</u>	<u>0.291</u>	<u>0.341</u>	
	<u>0.420</u>	<u>0.446</u>	<u>0.435</u>	<u>0.461</u>	<u>0.427</u>	<u>0.429</u>	<u>0.373</u>	<u>0.394</u>	
	<u>0.390</u>	<u>0.421</u>	<u>0.363</u>	<u>0.406</u>	<u>0.354</u>	<u>0.384</u>	<u>0.269</u>	<u>0.325</u>	
Time-Adapter	<b>0.352</b>	<b>0.393</b>	<b>0.285</b>	<b>0.377</b>	<b>0.285</b>	<b>0.340</b>	<b>0.173</b>	<b>0.262</b>	
	<b>0.383</b>	<b>0.414</b>	<u>0.351</u>	<u>0.390</u>	<u>0.332</u>	<u>0.369</u>	<u>0.234</u>	<u>0.302</u>	
	<b>0.399</b>	<b>0.425</b>	<u>0.376</u>	<u>0.413</u>	<u>0.366</u>	<u>0.392</u>	<u>0.291</u>	<u>0.337</u>	
	<b>0.417</b>	<b>0.446</b>	<u>0.416</u>	<u>0.446</u>	<u>0.421</u>	<u>0.426</u>	<u>0.373</u>	<u>0.389</u>	
	<b>0.388</b>	<b>0.420</b>	<u>0.357</u>	<u>0.407</u>	<u>0.351</u>	<u>0.382</u>	<u>0.268</u>	<u>0.323</u>	
		Time-CMA							
		ETTh1		ETTh2		ETTm1		ETTm2	
		MSE	MAE	MSE	MAE	MSE	MAE	MSE	MAE
Baseline	0.393	0.414	0.339	0.378	0.340	0.380	0.191	0.274	
	0.435	0.437	0.421	0.425	0.379	0.407	0.257	0.316	
	0.472	0.453	0.452	0.452	0.405	0.413	0.313	<b>0.350</b>	
	0.482	0.479	0.452	0.462	0.472	0.450	<b>0.416</b>	<b>0.407</b>	
	0.446	0.446	0.416	0.429	0.399	0.413	0.294	0.337	
TSCC	<u>0.377</u>	<u>0.396</u>	<b>0.299</b>	<u>0.347</u>	<u>0.311</u>	<u>0.352</u>	<u>0.173</u>	<u>0.256</u>	
	<u>0.429</u>	<u>0.424</u>	<u>0.377</u>	<u>0.395</u>	<u>0.360</u>	<u>0.381</u>	<u>0.242</u>	<u>0.301</u>	
	<u>0.468</u>	<u>0.444</u>	<u>0.415</u>	<u>0.426</u>	<u>0.396</u>	<u>0.405</u>	<u>0.307</u>	0.323	
	<u>0.474</u>	<u>0.471</u>	<u>0.424</u>	<u>0.443</u>	<u>0.464</u>	<u>0.444</u>	<u>0.416</u>	<u>0.407</u>	
	<u>0.437</u>	<u>0.434</u>	<u>0.379</u>	<u>0.403</u>	<u>0.383</u>	<u>0.396</u>	<u>0.285</u>	<u>0.322</u>	

Table 9: The results were conducted in the ETTh1, ETTh2, ETTm1, and ETTm2 datasets. The **Baseline** represents our reproduced results, which differ from those in the original paper. Under the same parameters, we added TSCC and Time-Adapter. The forecasting horizons were set to {96, 192, 336, 720}.